CMS Physics Analysis Summary

Contact: cms-pag-conveners-exotica@cern.ch 2012/07/13

Search for leptonic decays of W$'$ bosons in pp collisions at $\sqrt{s} = 8\,\mathrm{TeV}$

The CMS Collaboration

Abstract

A search for a new heavy gauge boson W$'$ decaying to an electron or muon and a low mass neutrino is presented. This analysis uses 2012 data corresponding to an integrated luminosity of 3.7 fb^{-1}, collected using the CMS detector in pp collisions at a centre-of-mass energy of 8 TeV at the LHC. No significant excess of events above the standard model expectation is found in the transverse mass distribution of the lepton-neutrino system. Mass exclusion limits at 95% CL for a SM-like W$'$ boson are determined. These results are also interpreted in the framework of split universal extra dimensions and exclusion limits on Kaluza–Klein W^2_{KK} states are set. Another reinterpretation of the channel W$' \rightarrow \mu\nu$ is performed in terms of compositeness with preons being fundamental constituents of fermions. A limit on the preon binding energy Λ, which would manifest itself as a four-fermion contact interaction, is set.

1 Introduction

This physics analysis summary describes a search for a new heavy gauge boson W', with proton-proton collision data collected from March until June of 2012 with the Compact Muon Solenoid (CMS) detector [1] at the LHC at a centre-of-mass energy of 8 TeV. The dataset corresponds to an integrated luminosity of $3.7\,\mathrm{fb}^{-1}$. We search for an excess of events with a charged lepton (an electron or muon) and a neutrino in the final state. The interpretation of the results is provided in the context of three theoretical models, the sequential standard model W', split UED and four-fermion contact interaction.

Similar searches were performed by CMS using LHC data at 7 TeV [2–4]. More details of the analysis strategy can be found in these earlier publications.

2 Physics models

New heavy gauge bosons such as the W' and Z' are predicted by various extensions of the standard model (SM). In the sequential standard model (SSM) [5], the W' boson is considered to be a heavy analogue of the W. It is assumed to be a narrow resonance with decay modes and branching fractions similar to those of the W, with the addition of the $t\bar{b}$ channel that becomes relevant for W' masses above 180 GeV. Interference between the W' and W is assumed to be negligible. If the W' is heavy enough to decay to top and bottom quarks, the predicted branching fraction is about 8.5% for each of the two leptonic channels studied in the present analysis. Under these assumptions, the width of a 1 TeV W' is about 33 GeV. Decays of the W' into WZ di-bosons are usually suppressed in this model.

The assumptions of the SSM were used in previous searches in leptonic channels at the Tevatron [6, 7] and the LHC [2–4, 8, 9]. Interference as studied in our previous publication [4] could not be considered since the simulated samples were not yet available.

The leptonic final states under study may also be interpreted in the framework of universal extra dimensions (UED) with bulk fermions, or split-UED [10, 11]. This is a model based on an extended space-time with an additional compact fifth dimension of radius R. In this model all SM particles have corresponding Kaluza–Klein (KK) partners, for instance W_{KK}^{n}, where n denotes the n-th KK excitation mode. Only KK-even modes of W_{KK}^{n} couple to SM fermions, owing to KK-parity conservation. Modes with $n \geq 4$ are not expected to be accessible at the present LHC conditions. Hence the only mode considered is n=2. Under this assumption, the decay to leptons is kinematically identical to the sequential SM-like W' decay, and the observed limits obtained from the $W' \to e\nu$ and $W' \to \mu\nu$ searches can directly be reinterpreted in terms of the W_{KK}^{n} mass.

The UED parameter space is defined by two parameters $[1/R, \mu]$ with μ being the bulk mass parameter of the fermion field in five dimensions. In the split UED model the parameter μ is assumed to be non-zero following [10, 11], thus increasing the cross sections sufficiently to allow observation by LHC experiments.

Another reinterpretation of the $W' \to \mu\nu$ final state is possible in terms of a four-fermion contact interaction. Motivated by the observation of mass hierarchies in the fermion sector, the basic model assumption is that quarks and leptons are composite objects of fundamental constituents called preons [12]. At energies much lower than their binding energy, typically called Λ, the quark and lepton compositeness would manifest itself as a four-fermion contact interaction. The contact interaction between two quarks, a neutrino and a charged lepton is described by the Helicity-non-Conserving model [13]. The corresponding cross-section is proportional to the square of the center-of-mass energy and to Λ^{-4}. In the Helicity-non-Conserving model there is no interference of the final state with the standard model W because of their different chiral structure. No limit has yet been set in the muon channel on Λ in the Helicity-Non-Conserving model. CDF has set a limit on the preon binding energy to $\Lambda = 2.81$ TeV [14] in the electron channel.

3 Event selection

Candidate events with at least one high-transverse-momentum (p_T) lepton were selected using single-muon (with $p_T > 40$ GeV) and single-electron (with $p_T > 85$ GeV) triggers. For both channels the offline p_T cut is 5 GeV higher, which does not impair the search in the high M_T region while keeping maximal statistics at the low and medium M_T control regions.

Muons were reconstructed by combining tracks from the inner tracker and the outer muon system, requiring at least one pixel hit, hits in nine tracker layers and segments in two muon stations. Each segment has multiple hits owing to the multilayer geometry of muon chambers. Since segments are typically found in consecutive muon stations separated by thick layers of iron, the latter requirement significantly reduces the amount of hadronic punch-through. The transverse impact parameter $|d_0|$ of the muon track with respect to the interaction point is required to be less than 0.02 cm, in order to reduce the cosmic-ray muon background. Furthermore, the muon is required to be isolated within a $\Delta R \equiv \sqrt{\Delta\phi^2 + \Delta\eta^2} < 0.3$ cone around its direction. Muon isolation requires that the scalar sum of the transverse momenta of all tracks originating at the interaction vertex, excluding the muon, is less than 15% of its p_T. An additional requirement is that there be no second muon in the event with $p_T > 25$ GeV to reduce the Z, Drell-Yan and cosmic ray muon backgrounds.

Electrons were reconstructed as isolated objects in the electromagnetic calorimeter, with additional requirements on the shower shape and the ratio of hadronic to electromagnetic deposited energies. The electrons were required to have at least one inner tracker hit, a transverse energy greater than 90 GeV, and were required to be isolated in a cone of radius $\Delta R \equiv \sqrt{\Delta\eta^2 + \Delta\phi^2} < 0.3$ around the electron candidate direction, both in the tracker and in the calorimeter. In the tracker, the sum of the p_T of the tracks, excluding tracks within an inner cone of 0.04, was required to be less than 5 GeV. For the isolation using calorimeters, the total transverse energy in the barrel, excluding deposits associated to the electron, was required to be less than $0.03 \cdot E_T^{\mathrm{ele}} + 2.0$ GeV.

The main observable in this search is the transverse mass M_T of the lepton-E_T^{miss} system, calculated as

$$M_T = \sqrt{2 \cdot p_T^{\ell} \cdot E_T^{\mathrm{miss}} \cdot (1 - \cos \Delta\phi_{\ell,\nu})} \quad (1)$$

where $\Delta\phi_{\ell,\nu}$ is the azimuthal opening angle between the charged lepton's transverse momentum (p_T^{ℓ}) and E_T^{miss} direction. The neutrino is not detected directly, but gives rise to experimentally observed missing transverse energy (E_T^{miss}). This quantity was determined using a particle-flow technique [15], an algorithm designed to reconstruct a complete list of distinct particles using all the subcomponents of the CMS detector.

In W$'$ decays, the lepton and E_T^{miss} are expected to be almost back-to-back in the transverse plane, and balanced in transverse energy. Candidate events were therefore selected through a requirement on the ratio of the lepton p_T and the E_T^{miss}, $0.4 < p_T/E_T^{\mathrm{miss}} < 1.5$. A requirement was also imposed on the angular difference in the transverse plane of the lepton and E_T^{miss} direction, $\Delta\phi_{\ell,\nu} > 0.8 \times \pi$. No selection is made on jets. After these selections, the average

W′ signal efficiency for masses ranging from about 0.7 TeV to 2.5 TeV in simulated events was found to be around 70% in both channels, including the roughly 90% geometrical acceptance corresponding to a requirement of $|\eta_\mu| < 2.1$ for muons, and $|\eta_e| < 1.442$ or $1.56 < |\eta_e| < 2.5$ for electrons. For higher W′ masses up to 4 TeV the signal efficiencies slowly decrease to 50% due to an increasing fraction of W′ off their mass shell. The transverse mass distributions after these selections are shown in Figure 1.

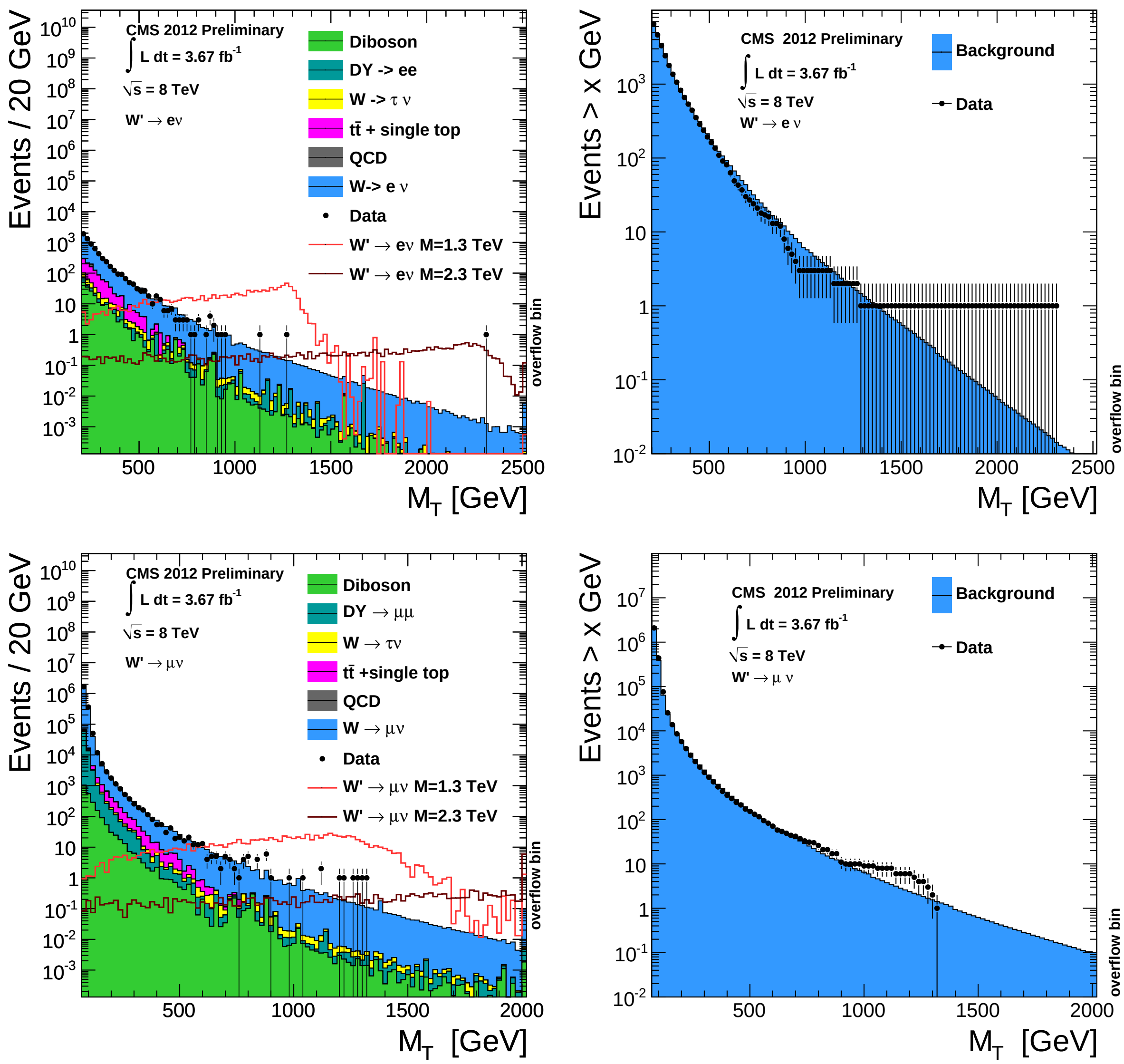

Figure 1: Observed transverse mass distributions (left) and their cumulative distributions (right) for the electron (upper row) and muon (lower row) channels. The significance of the slight excess in the muon channel is 1.1 sigma for M_T >1.1 TeV. Simulated signal distributions for a W′ are also shown, including detector resolution effects. The simulated background labeled as 'di-boson' includes WW, ZZ and WZ contributions.

4 Signal and background simulation

Several large samples of simulated events were used to evaluate signal and background efficiencies. The generated events were processed through a full simulation of the CMS detector based on GEANT4 [16, 17], a trigger emulation, and the event reconstruction chain.

W' signals are generated at leading order (LO) with PYTHIA using the CTEQ6L1 parton distribution functions (PDF) [18]. Mass-dependent K-factors for the next-to-next-to-leading order (NNLO) correction were calculated with FEWZ [19, 20].

Signal samples for four-fermion contact interaction (Helicity-Non-Conserving model [13]) are produced with PYTHIA at leading order. For 2012 three points are available at the time of this analysis corresponding to Λ = 4, 7 and 9 TeV.

The primary source of background for all these signals is the off-peak, high transverse mass tail of the standard model $W \rightarrow \ell\nu$ decays. Other important backgrounds arise from QCD multijet, $t\bar{t}$, and Drell–Yan events. Di-bosons (WW, WZ, ZZ) decaying to electrons, muons, or taus were also considered. The event samples for the electroweak background processes $W \rightarrow \ell\nu$ and $Z \rightarrow \ell\ell$ ($\ell = e, \mu, \tau$) were produced using PYTHIA. NNLO cross sections were accounted for via a single K-factor of 1.32 for the W, and mass-dependent K-factors, ranging from 1.28 to 1.23, for the Z. The PYTHIA generator was also used for QCD multijet events. The $t\bar{t}$ events were generated with MADGRAPH in combination with PYTHIA, and the newly-calculated NNLL (next-to-leading-order including the leading logarithms of NNLO) cross section was applied [21]. All other event samples were normalized to the integrated luminosity of the recorded data, using calculated NNLO cross sections. The only exceptions were the di-boson and QCD samples, for which the NLO and LO cross sections were used respectively. We note that multijet background is largely suppressed by the event selection requirements. The simulation of pile-up is included in all event samples by superimposing minimum bias interactions onto the main background processes.

The background can be determined with two methods. Method (A) uses data and fits the sideband of the M_T distribution in the range 200 GeV- 600 GeV. Method (B) fits the full M_T distribution (for M_T >200 GeV) in simulation and normalizes it to data in the region 200 GeV $< M_T <$ 500 GeV. In both cases a function, of the form

$$f(M_T) = \frac{a}{(M_T + b)^c} \tag{2}$$

is used to estimate the expected number of SM background events for all transverse mass bins. To determine the uncertainty introduced by this method, in addition to statistical errors on the fit parameters, two alternative functions were fitted:

$$f(M_T) = \frac{a}{(M_T^2 + b \cdot M_T + c)^d} \tag{3}$$

$$f(M_T) = \frac{a(1 + M_T)^b}{(M_T^{c+d \cdot \ln M_T})} \tag{4}$$

The largest difference in the background prediction with respect to the original fit was taken as a systematic uncertainty.

5 Results and limits

A $W^{'} \rightarrow e\nu$ or $W^{'} \rightarrow \mu\nu$ signal is expected to manifest itself as an excess over the SM expectation in the tail of the M_T distribution. The expected numbers of signal events for various $W^{'}$ masses along with the number of SM background events are shown in Tables 1 and 2 for the electron and muon channel, respectively. Both channels use the fit to the full simulated M_T distribution to determine the expected number of SM background events. This method is more precise yielding smaller uncertainties on the background prediction compared to the extrapolation of the data sideband fit. Also shown are the the number of observed events and the NNLO $W^{'}$ theoretical cross-sections which are assumed to be equal in both channels following the SSM predictions.

Table 1: Electron channel: expected numbers of signal and background events, the number of observed events, the corresponding cross-sections, and expected and observed limits for different $W^{'}$ masses and search windows.

$W^{'}$ mass (GeV)	M_T (GeV)	N_{sig} (Events)	N_{bkg} (Events)	N_{data} (Events)	σ_{theor} (fb)	Exp. Limit (fb)	Obs. Limit (fb)
700	550	8200 ± 1200	106 ± 12	96	5800	23	19
1100	850	1160 ± 170	15.5 ± 4.6	12	780	8.5	6.3
1700	1200	110 ± 12	3.25 ± 1.9	2	73	3.9	3.1
2300	1700	11.8 ± 1.4	0.63 ± 0.59	1	9.8	2.7	3.8
2500	1700	6.15 ± 0.69	0.63 ± 0.59	1	5.4	2.8	3.9
2600	1700	4.85 ± 0.47	0.63 ± 0.59	1	4.1	2.7	3.8
2800	1750	2.41 ± 0.21	0.54 ± 0.53	1	2.4	3.1	4.5
3000	1700	1.317 ± 0.089	0.63 ± 0.59	1	1.5	3.7	5.1
3300	1700	0.510 ± 0.035	0.63 ± 0.59	1	0.85	5.3	7.4
3500	1700	0.303 ± 0.025	0.63 ± 0.59	1	0.63	6.6	9.0
4000	1400	0.105 ± 0.015	1.6 ± 1.2	1	0.33	13	13

Table 2: Muon channel: expected numbers of signal and background events, the number of observed events, the corresponding cross-sections, and expected and observed limits for different $W^{'}$ masses and search windows.

$W^{'}$ mass (GeV)	M_T (GeV)	N_{sig} (Events)	N_{bkg} (Events)	N_{data} (Events)	σ_{theor} (fb)	Exp. Limit (fb)	Obs. Limit (fb)
700	550	7400 ± 1000	90.8 ± 9.4	107	5800	24	30
1100	850	1050 ± 160	12.7 ± 3.0	21	780	8.3	14
1700	1150	109 ± 11	3.1 ± 1.2	6	73	3.8	6.1
2300	1350	14.04 ± 0.94	1.41 ± 0.69	0	9.8	2.9	2.1
2500	1350	7.80 ± 0.59	1.41 ± 0.69	0	5.4	2.9	2.1
2600	1350	5.46 ± 0.36	1.41 ± 0.69	0	4.1	3.2	2.2
2800	1350	2.91 ± 0.15	1.41 ± 0.69	0	2.4	3.4	2.5
3000	1350	1.519 ± 0.092	1.41 ± 0.69	0	1.5	4.2	3.1
3300	1350	0.614 ± 0.028	1.41 ± 0.69	0	0.85	5.8	4.3
3500	1350	0.346 ± 0.032	1.41 ± 0.69	0	0.63	7.6	5.5
4000	1350	0.105 ± 0.012	1.41 ± 0.69	0	0.33	13	9.8

No significant excess has been observed in the data and upper limits on the production cross section times the branching fraction $\sigma_{W'} \times \mathcal{B}(W^{'} \rightarrow \ell\nu)$, with $\ell = e$ or μ are set. The observed highest transverse mass events have $M_T = 2.3$ TeV in the electron channel, and $M_T = 1.3$ TeV in the muon channel. The expected and observed limits for different W′ masses and search windows are shown in Tables 1 and 2 and Figure 2. Using the central value of the theoretical cross section times the branching fraction, we exclude at 95% confidence level (CL) the existence of a W′ with SM-like couplings of masses less than 2.75 TeV (compared with an expected limit of 2.65 TeV) in the muon and 2.60 TeV (compared to 2.70 TeV expected) in the electron channel. In the latter the observed limit is below the expected due to the event at M_T =2.3 TeV.

Cross-section limits were derived using a Bayesian method [22] with a uniform prior probability distribution for the signal cross section. The number of data events above an optimized transverse mass threshold M_T^{min} was compared to the expected number of signal and background events. Systematic uncertainties on the signal and background yield were included via nuisance parameters with a log-normal prior distribution. The M_T^{min} threshold was optimized for the best expected exclusion limit, a procedure used in previous analyses [3, 4].

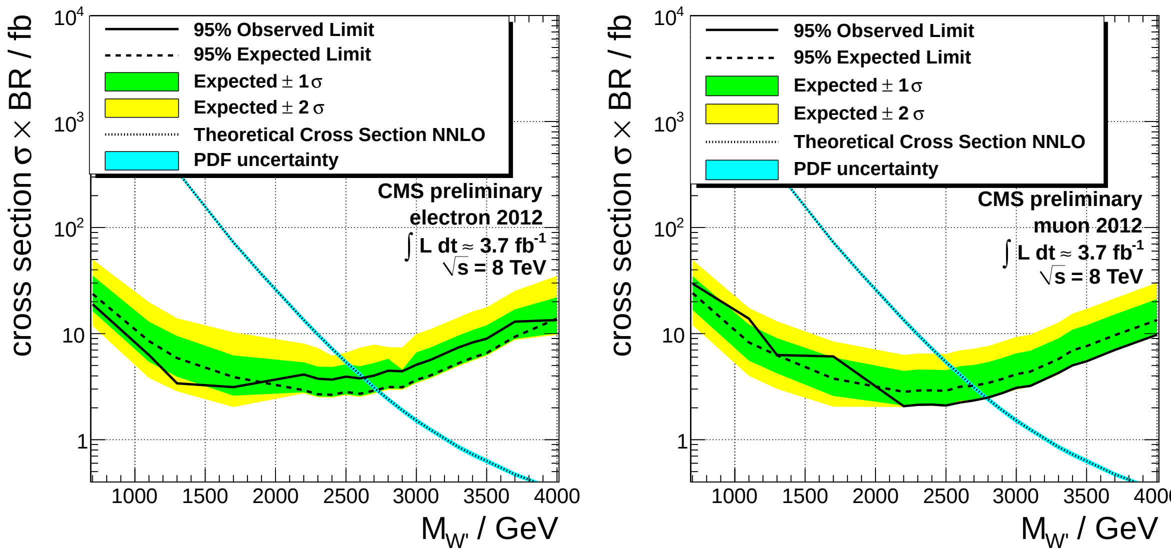

Figure 2: Upper cross section limits at 95% confidence level on $\sigma(W') \times B(W' \to \ell\nu)$ with $\ell = e$ (left) and $\ell = \mu$ (right). The one (two) sigma uncertainty bands are shown in green (yellow). The theoretical cross section, is displayed with a mass-dependent NNLO K-factor.

Table 3: Limits from the combination of 2012 electron and muon channel.

$M_{W'}$	700	1100	1300	1700	2200	2300	2400	2500	2600	2700
$M_T^{lower}(e,2012)$	550	850	1000	1200	1700	1700	1700	1700	1700	1700
$M_T^{lower}(\mu,2012)$	550	850	900	1150	1350	1350	1350	1350	1350	1350
Observed limit / fb	16.77	6.71	2.78	2.96	1.57	1.52	1.55	1.57	1.61	1.70
Expected limit / fb	17.40	5.52	4.12	2.60	1.95	1.91	1.90	1.94	1.98	2.12

$M_{W'}$	2800	2900	3000	3100	3300	3400	3500	3700	4000
$M_T^{lower}(e,2012)$	1750	1750	1700	1700	1700	1700	1700	1700	1400
$M_T^{lower}(\mu,2012)$	1350	1350	1350	1350	1350	1350	1350	1350	1350
Observed limit / fb	1.86	1.97	2.19	2.34	3.05	3.59	3.98	5.28	6.18
Expected limit / fb	2.27	2.37	2.67	2.90	3.79	4.40	4.87	6.58	9.08

The results of the individual channels are combined assuming independent uncertainties (no correlation) apart from the luminosity uncertainty which is fully correlated. Combining both

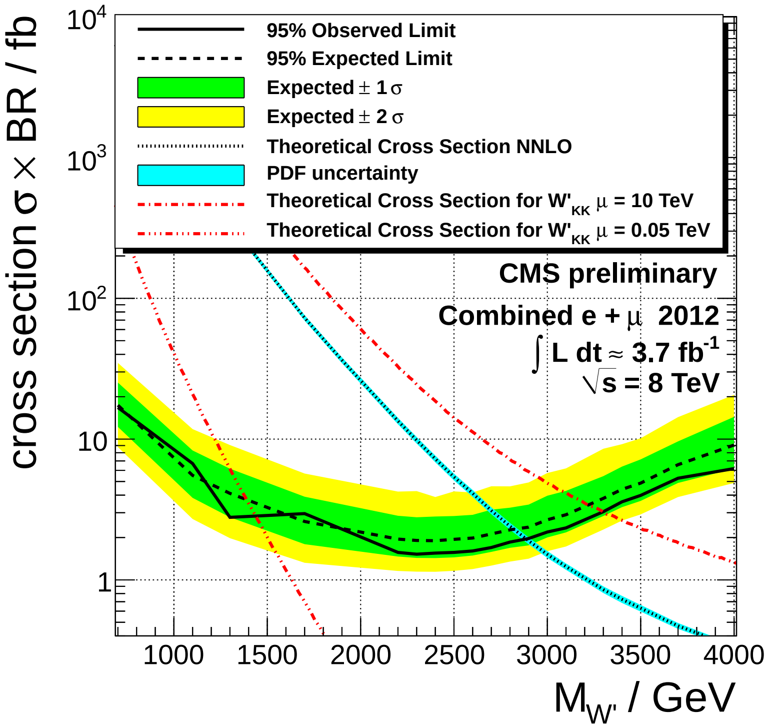

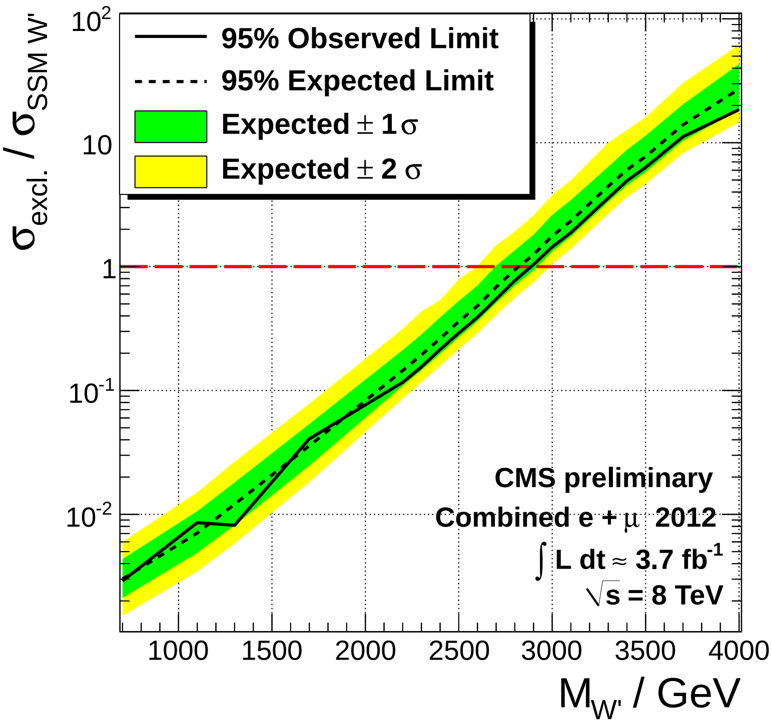

Figure 3: Combination of 2012 electron and muon channel. The limits are derived with a Bayesian method. On top the conventional style displaying the excluded $W^{'}$ cross section. On the bottom the result is shown in a different style, where the excluded cross section is divided by the $W^{'}$ SSM cross section.

channels, which is equal to doubling the statistics, the limit increases to 2.85 TeV. With 5 fb^{-1} of data at $\sqrt{s} = 7$ TeV the exclusion limit was at 2.5 TeV when combining both channels [4]. Figure 3 displays the excluded W$'$ cross section times branching ratio as a function of the W$'$ mass. The corresponding values are summarized in Table 3.

To further increase the sensitivity of the search, the 3.7 fb^{-1} taken in 2012 at a center-of-mass energy of 8 TeV can be combined with the 5 fb^{-1} of 2011 data at center-of-mass energy of 7 TeV. Owing to the different cross sections, a simple limit on the excluded cross section cannot be derived and rather the ratio of the total number of observed events with respect to the predicted number SSM W$'$ events is examined. As a common quantity for all channels a signal strength modifier $\theta = \sigma_{\text{excluded}}/\sigma_{\text{SSM W}'}$ is introduced. I.e., the exclusion of $\theta = 1$ corresponds to the exclusion of a sequential standard model W$'$ boson. The combination of electron and muon channels for 2011 and 2012 yields a limit on a SSM W$'$ of 2.85 TeV as shown in Figure 4, no further improvement over the 2012 sensitivity. All limits are summarized in Table 4.

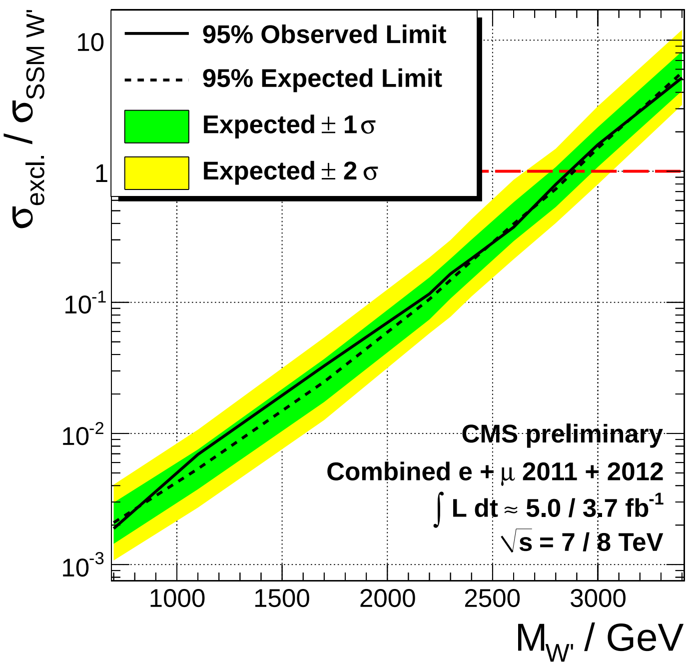

Figure 4: Combination of 2011 and 2012, electron and muon channel using 5.0 fb^{-1} for 7 TeV 2011 and 3.7 fb^{-1} of 8 TeV 2012 data. The limits are derived with a Bayesian method. Plotted is the signal strength modifier $\theta = \sigma_{\text{excluded}}/\sigma_{\text{SSM W}'}$ depending on the W$'$ mass. All W$'$ mass points below the ratio θ=1, shown as a red dashed line, are excluded in the sequential standard model.

Table 4: List of limits for the electron and muon channel as well as their combinations.

W$'$ Channel(s)	Luminosity / fb^{-1}	Observed SSM W$'$ lower mass limit / TeV	Expected SSM W$'$ lower mass limit / TeV
e 2012	3.7	2.60	2.70
μ 2012	3.7	2.75	2.65
$e + \mu$ 2012	3.7	2.85	2.80
$e + \mu$ 2011 + 2012	5.0 + 3.7	2.85	2.85

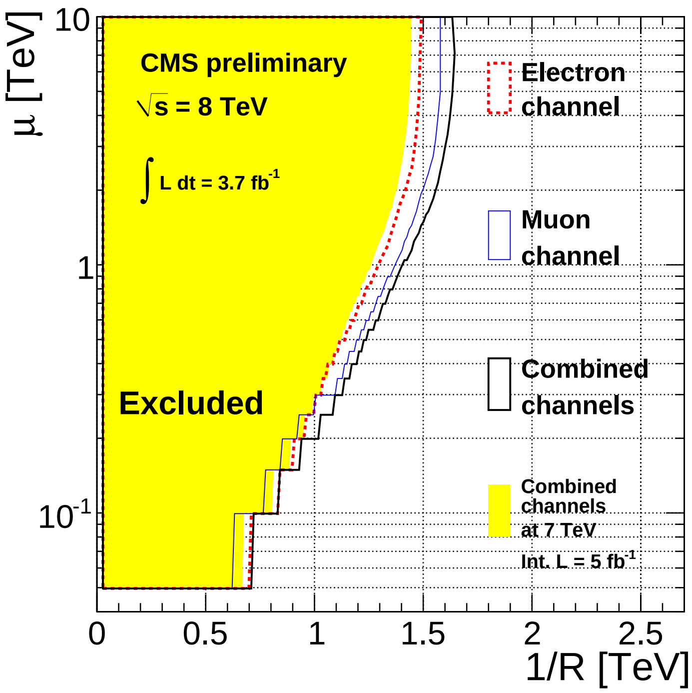

Figure 5: 95% confidence limits on the split-UED parameters μ and $1/R$ derived from the W' mass limits taking into account the corresponding width of the W^2_{KK}. The limit for the electron (red dotted line) and the muon channel (blue line) individually along with their combination in 2012 is compared to the CMS 2011 combined result (yellow). The W^2_{KK} is the lowest state that can couple to SM fermions and has the same final state as the SM-like W'. Since it has even parity it can be produced singly.

The observed limits illustrated in Figure 2 can be reinterpreted in terms of the W^2_{KK} mass, as shown in the same figure for values of the bulk mass parameters $\mu = 0.05$ TeV and $\mu = 10$ TeV. These lower limits on the mass can be directly translated to bounds on the split-UED parameter space $[1/R, \mu]$ as shown in Figure 5.

Another reinterpretation can be done in terms of four-fermion contact interaction (Helicity-Non-Conserving model), providing a limit on the preon binding energy scale Λ. Statistical interpretation is identical to W', using a Bayesian approach with a uniform prior [22] requiring 95% confidence level. The expected and observed limits for Λ and search windows are shown in Tables 5 and Figure 6. The limit on Λ is calculated to be 8.7 TeV. For $\Lambda = 4, 7$ and 9 TeV signal efficiencies, including the detector acceptance, are evaluated to be 77%, 78% and 79%. For other values of Λ an interpolation was used to estimate the efficiencies.

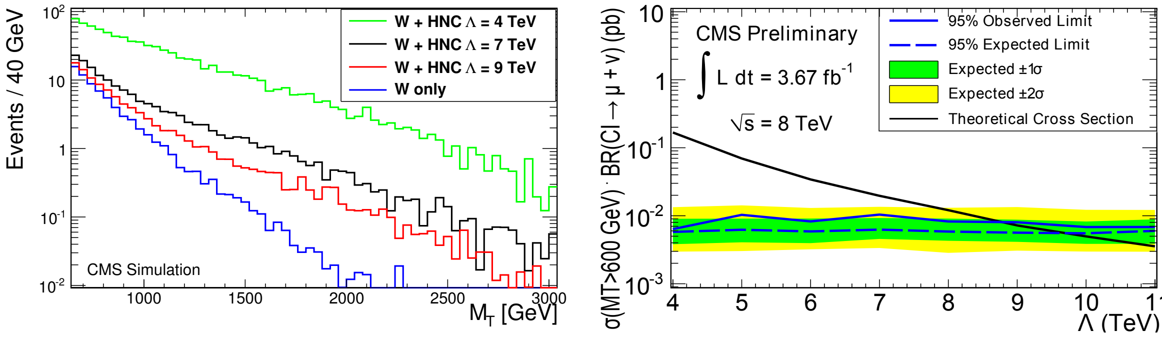

Figure 6: Left: Signal distribution of a contact interaction in the muon channel on generator level (SM W included). right: Bayesian limit for a contact interaction in the muon channel based on 3.7 fb^{-1} of data. The background prediction is derived from a fit to the simulated M_T distribution.

Table 5: Expected numbers of signal and background events for contact interaction in the muon channel. For a given minimum M_T the background prediction is identical to $W' \to \mu\nu$ as shown in Table 2. Also shown are the number of observed events, the corresponding signal cross-sections (for $\sqrt{s} = 8$ TeV), and expected and observed limits for preon binding energy scales Λ and the corresponding search windows.

Λ (GeV)	M_T (GeV)	N_{sig} (Events)	N_{bkg} (Events)	N_{data} (Events)	$\sigma_{theor}(MT > 600$ GeV) (fb)	Exp. Limit (fb)	Obs. Limit (fb)
4000	900	261±20	10.7±2.6	11	167.60	5.78	6.36
5000	850	122±9	13.9±3.1	21	69.53	6.22	10.31
6000	1000	42.6±4.4	6.5±1.9	9	34.18	5.88	8.25
7000	1050	19.6±1.9	5.2±1.7	9	17.71	6.25	10.40
8000	1000	15.2±1.6	6.5±1.9	9	12.07	5.85	8.24
9000	1000	9.20±0.92	6.5±1.9	9	6.97	5.64	8.02
10000	950	7.49±0.78	8.3±2.3	10	4.97	5.52	6.82
11000	950	5.38±0.56	8.3±2.3	10	3.55	5.99	6.82

6 Summary

A search for an excess of events with a final state consisting of a charged lepton (electron or muon) and significant missing transverse momentum has been performed, using 3.5 fb^{-1} of $\sqrt{s} = 8$ TeV pp collision data. No significant excess over the SM expectation was observed in the distribution of transverse mass. A SSM W' with a mass of less than 2.85 TeV has been excluded at 95% CL with the 2012 data. Combining the 2012 result with the 2011 data the W' exclusion limit does not improve further due to the higher center-of-mass energies in 2012.

An interpretation of the search results has also been made in a specific framework of universal extra dimensions with bulk mass fermions. The second Kaluza–Klein excitation W^2_{KK} has been excluded for masses below 1.4 TeV, assuming a bulk mass parameter μ of 0.05 TeV or masses below 3.3 TeV for μ=10 TeV.

Another reinterpretation in terms of four-fermion contact interaction (Helicity-non-conserving model) yields a limit for the preon binding energy scale Λ of 8.7 TeV.

7 Event displays

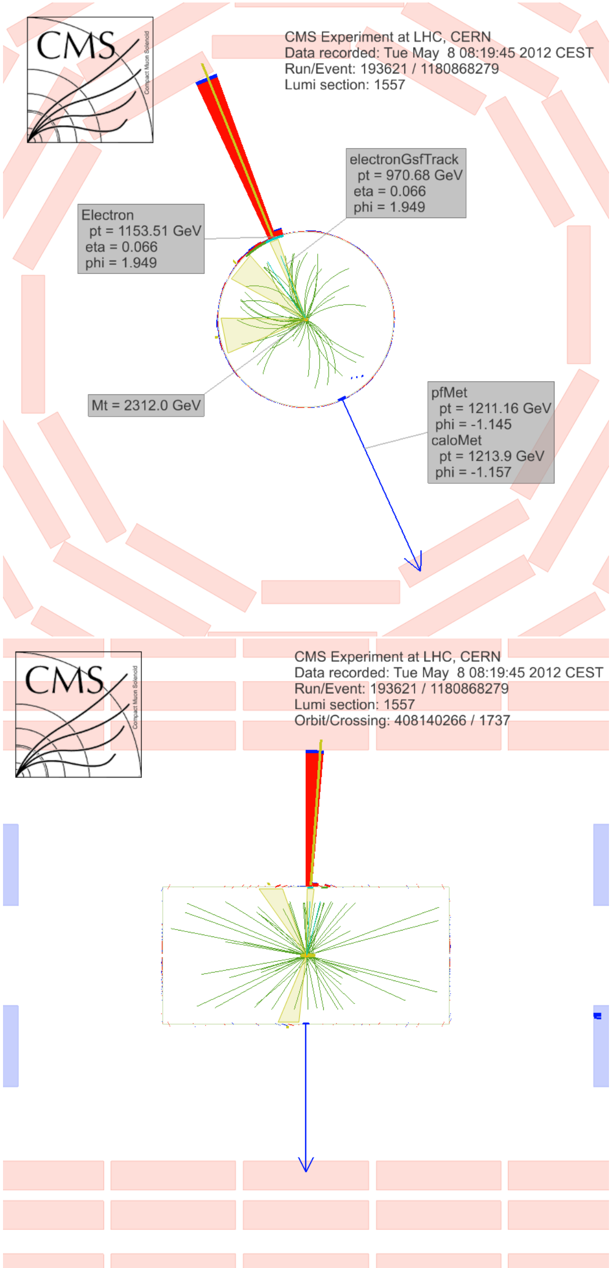

Figure 7: Event with the highest transverse mass of 2.3 TeV in the electron channel: ρ-ϕ view (top) and ρ-z view (bottom).

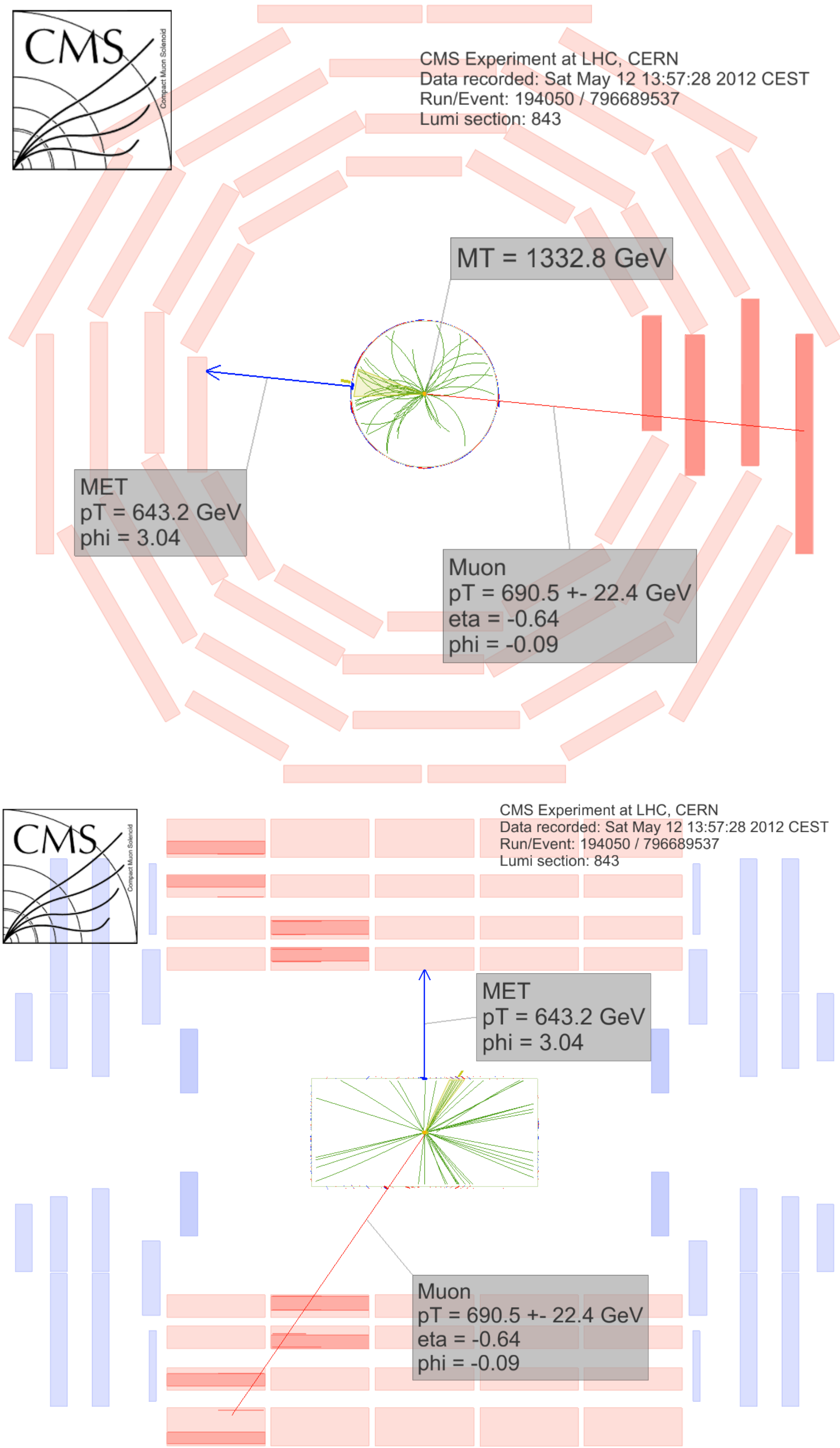

Figure 8: Event with the highest transverse mass of 1.3 TeV in the muon channel: ρ-ϕ view (top) and ρ-z view (bottom).

References

[1] CMS Collaboration, "The CMS experiment at the CERN LHC", *JINST* **03** (2008) S08004, doi:10.1088/1748-0221/3/08/S08004.

[2] CMS Collaboration, "Search for a heavy gauge boson W′ in the final state with an electron and large missing transverse energy in pp collisions at $\sqrt{s} = 7$ TeV", *Phys. Lett. B* **698** (2011) 21, doi:10.1016/j.physletb.2011.02.048, arXiv:1012.5945.

[3] CMS Collaboration, "Search for a W' boson decaying to a muon and a neutrino in pp collisions at $\sqrt{s} = 7$ TeV", *Phys. Lett. B* **701** (2011) 160, doi:10.1016/j.physletb.2011.05.048, arXiv:1103.0030.

[4] CMS Collaboration Collaboration, "Search for leptonic decays of $\mathrm{W}^{'}$ bosons in pp collisions at sqrt(s) = 7 TeV", *JHEP* **accepted for publication** (2012) arXiv:1204.4764v1.

[5] G. Altarelli, B. Mele, and M. Ruiz-Altaba, "Searching for New Heavy Vector Bosons in $\mathrm{p\bar{p}}$ Colliders", *Z. Phys. C* **45** (1989) 109, doi:10.1007/BF01556677.

[6] CDF Collaboration, "Search for a New Heavy Gauge Boson W' with Electron + missing ET Event Signature in $p\bar{p}$ collisions at $\sqrt{s} = 1.96$ TeV", *Phys. Rev. D* **83** (2011) 031102, doi:10.1103/PhysRevD.83.031102, arXiv:1012.5145.

[7] D0 Collaboration, "Search for W' bosons decaying to an electron and a neutrino with the D0 detector", *Phys. Rev. Lett.* **100** (2008) 031804, doi:10.1103/PhysRevLett.100.031804, arXiv:0710.2966.

[8] ATLAS Collaboration, "Search for high-mass states with one lepton plus missing transverse momentum in proton-proton collisions at $\sqrt{s} = 7$ TeV with the ATLAS detector", *Phys. Lett. B* **701** (2011) 50, doi:10.1016/j.physletb.2011.05.043, arXiv:1103.1391.

[9] ATLAS Collaboration, "Search for a heavy gauge boson decaying to a charged lepton and a neutrino in 1 fb^{-1} of pp collisions at $\sqrt{s} = 7$ TeV using the ATLAS detector", *Phys. Lett. B* **705** (2011) 28, doi:10.1016/j.physletb.2011.09.093, arXiv:1108.1316.

[10] C.-R. Chen, M. M. Nojiri, S. C. Park et al., "Dark matter and collider phenomenology of split-UED", *JHEP* **09** (2009) 078, doi:10.1088/1126-6708/2009/09/078, arXiv:0903.1971.

[11] K. Kong, S. C. Park, and T. G. Rizzo, "Collider Phenomenology with Split-UED", *JHEP* **04** (2010) 081, doi:10.1007/JHEP04(2010)081, arXiv:1002.0602.

[12] K. A. H. Terazawa, M. Yasue and M. Hayashi, "Observable Effects of the Possible Substructure of Leptons and Quarks", *Phys. Lett.* **B112** (1982) 387, arXiv:hep-ph/1110.0713v1.

[13] K. Lane, F. Paige, T. Skwarnicki et al., "Simulations of supercollider physics", *Phys.Rept.* **278** (1997) 291–371, arXiv:hep-ph/9412280.

[14] CDF Collaboration Collaboration, "Search for quark lepton compositeness and a heavy W' boson using the $e\nu$ channel in $p\bar{p}$ collisions at $\sqrt{s} = 1.8$ TeV", *Phys.Rev.Lett.* **87** (2001) 231803, arXiv:hep-ex/0107008.

[15] CMS Collaboration, “Particle–Flow Event Reconstruction in CMS and Performance for Jets, Taus, and $E_{\mathrm{T}}^{\mathrm{miss}}$”, CMS Physics Analysis Summary CMS-PAS-PFT-09-001, (2009).

[16] GEANT4 Collaboration, “GEANT4 – a simulation toolkit”, *Nucl. Instrum. Meth. A* **506** (2003) 250, doi:10.1016/S0168-9002(03)01368-8.

[17] J. Allison et al., “GEANT4 developments and applications”, *IEEE Trans. Nucl. Sci.* **53** (2006) 270, doi:10.1109/TNS.2006.869826.

[18] J. Pumplin, D. R. Stump, J. Huston et al., “New generation of parton distributions with uncertainties from global QCD analysis”, *JHEP* **07** (2002) 012, doi:10.1088/1126-6708/2002/07/012, arXiv:hep-ph/0201195.

[19] R. Gavin, Y. Li, F. Petriello et al., “FEWZ 2.0: A code for hadronic Z production at next-to-next-to-leading order”, *Comput. Phys. Commun.* **182** (2011) 2388, doi:10.1016/j.cpc.2011.06.008, arXiv:1011.3540.

[20] R. Gavin, Y. Li, F. Petriello et al., “W physics at the LHC with FEWZ 2.1”, (2012). arXiv:1201.5896.

[21] N. Kidonakis and R. Vogt, “The Theoretical top quark cross section at the Tevatron and the LHC”, *Phys. Rev. D* **78** (2008) 074005, doi:10.1103/PhysRevD.78.074005, arXiv:0805.3844.

[22] Particle Data Group Collaboration, “Review of Particle Physics”, *J. Phys. G* **37** (2010) 075021, doi:10.1088/0954-3899/37/7A/075021. Chap. 33.